SUPPLEMENTAL FIGURES

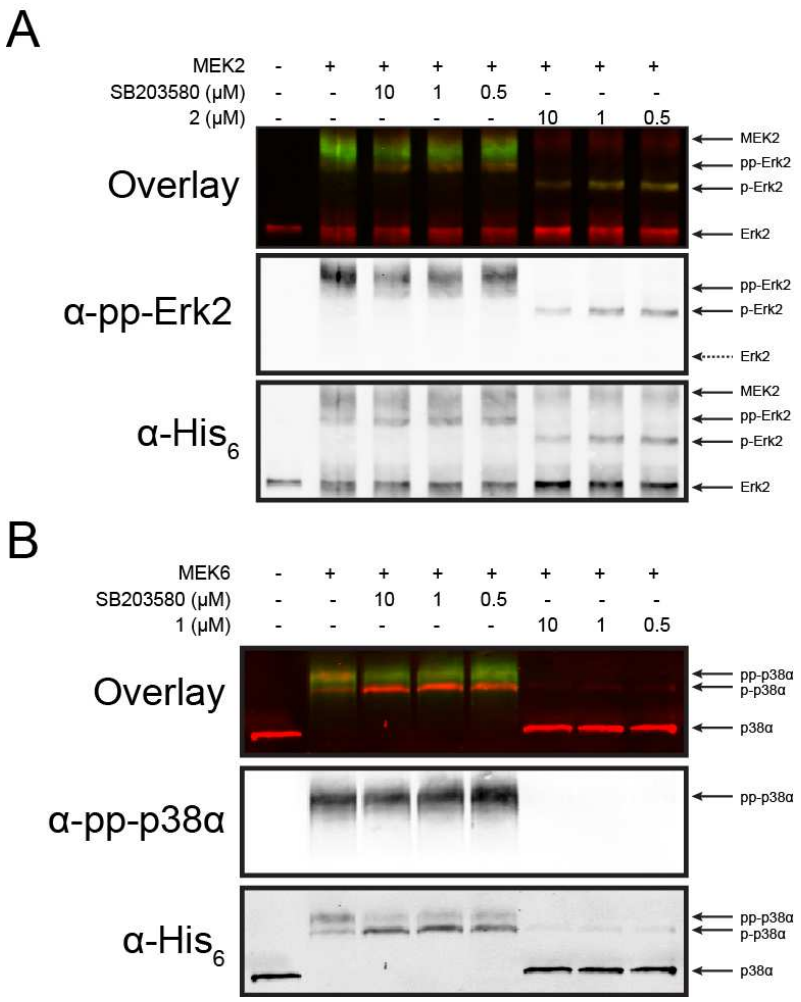

Figure S1, related to Figure 3. A. Activation inhibition analysis of $Erk2^{DS1}$ in the presence of inhibitor **2** or SB203580. The samples were run on a gel cast with PhosTag-acrylamide to separate phospho-isoforms, and the blot was probed with rabbit α-pp-Erk2 (Santa Cruz Biotechnology) and mouse α-His_6 (Abm). B. Activation inhibition analysis of p38α in the presence of inhibitor **1** or SB203580. The samples were run on a gel cast with PhosTag-acrylamide to separate phospho-isoforms, and the blot was probed with rabbit α-pp-p38α (Cell Signaling) and mouse α-His_6 (Abm).

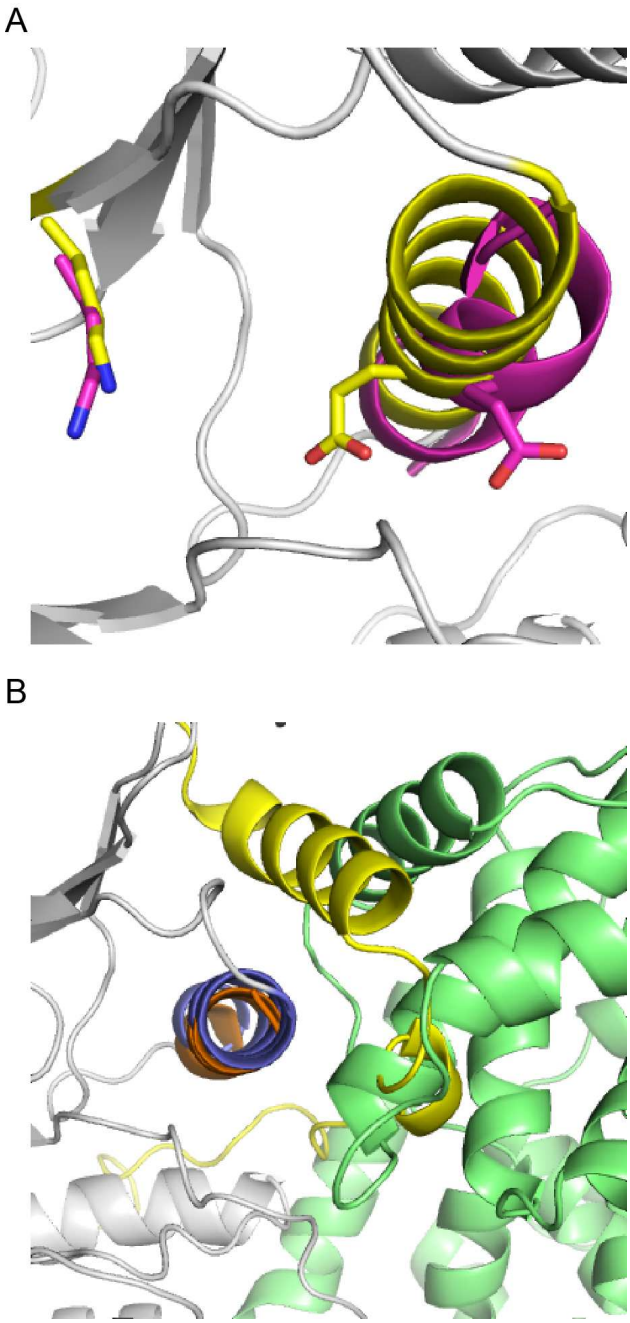

Figure S2, related to Figure 5. A. Superimposed structures of **3**-bound Erk2^{DS2} (gray and yellow) and Src bound to an analogue of **3** (magenta) (PDB ID: 4DGG). The residues which form a salt bridge in the active conformation are represented in stick form. B. Superimposed structures of **3**-bound Erk2^{DS2} (gray with helix αC in blue and C-terminal extension in yellow) and cyclin-bound Cdk2 (helix αC in orange and cyclin in green) (PDB ID: 1FIN).

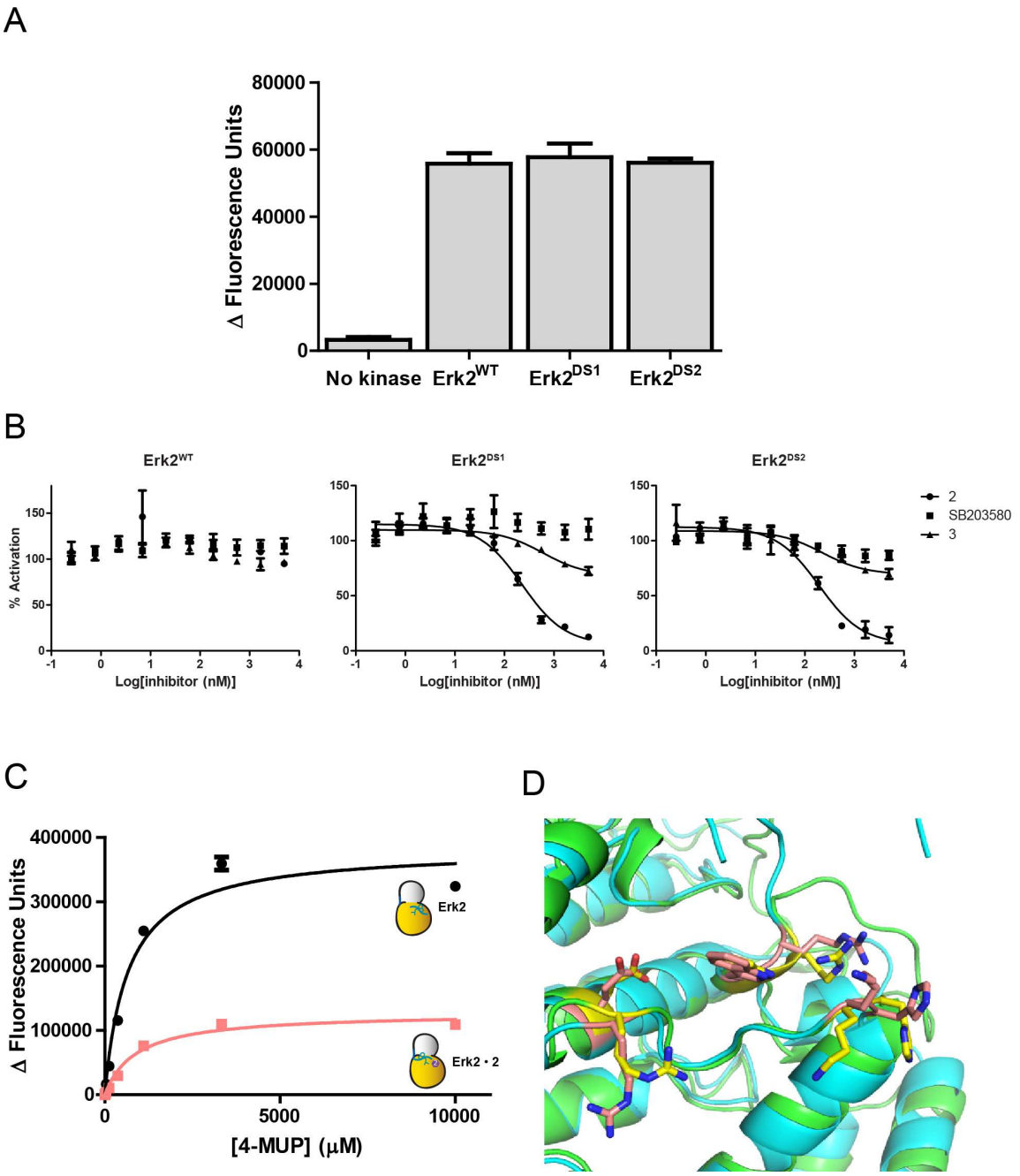

Figure S3, related to Figure 7. A. Increase in catalytic activity of DUSP6 upon addition of either Erk2 wild-type or inhibitor-sensitive mutants. The substrate used was 4-methylumbelliferyl phosphate (4-MUP). Background subtraction was performed using samples without kinase or DUSP6. B. Inhibition of Erk2-mediated DUSP6 activation. Ligands **2**, **3**, or SB203580 were titrated into unphosphorylated Erk2 wild-type or inhibitor-sensitive mutants. DUSP6 was then added to the reaction, followed by substrate 4-MUP. The phosphatase reaction was followed by fluorescence. The data were then fit to a curve, using zero inhibitor (DMSO) as the minimum possible level of inhibition and no Erk2 as the maximum. The EC_{50} values for ligand **2** were determined to be 230 ± 10 nM and 200 ± 10 nM for **2** against $Erk2^{DS1}$ and $Erk2^{DS2}$,

respectively. Partial inhibition (~30%) was observed for ligand **3**. C. Kinetics of the DUSP6/Erk2^{DS1} complex with different inhibitors. K_m[4-MUP] values were determined to be 670 ± 70 μM and 890 ± 100 μM for the apo and **2**-bound complexes, respectively. D. Structural alignment of Erk2 in the DFG-in (green, PDB ID: 1ERK) and DFG-out (cyan, PDB ID: 4I5H) conformations with residues forming the substrate binding domain shown as sticks in yellow and salmon, respectively. Error bars represent standard error of the mean (SEM) for three replicate measurements.

SUPPLEMENTAL TABLES

A.

	1	**2**	**SB302580**
K_i (nM)	6.4 ± 1.6	< 2	28 ± 7
EC_{50} (nM)	7.4 ± 0.9	30 ± 20	>10000

B.

	2		SB203580		3	
	K_i (nM)	**EC_{50} (nM)**	**K_i (nM)**	**EC_{50} (nM)**	**K_i (nM)**	**EC_{50} (nM)**
Erk2^{WT}	>10000	5000 ± 800	>10000	>10000	>10000	390 ± 40
Erk2^{DS1}	4.7 ± 0.3	42 ± 4	9.8 ± 1.1	< 20[a]	N/D	N/D
Erk2^{DS2}	< 2	N/D	< 2	N/D	133 ± 6	840 ± 30

Table S1, related to Figure 3. A. Enzymatic inhibition (K_i) and activation inhibition (EC_{50}) of p38α using the ligands shown in Figure 2B. K_i values for **1** and **2** were reported earlier.[1] EC_{50} values for **1** and SB203580 were determined by the present authors as a confirmation of data originally reported elsewhere.[2] B. Enzymatic inhibition (K_i) and activation inhibition (EC_{50}) of Erk2^{WT}, Erk2^{DS1}, and Erk2^{DS2} by inhibitors **2**, **3**, and SB203580. K_i values for **2** were previously reported.[1] [a]Inhibition of only 30% at saturating inhibitor concentrations. As ligand **3** does not inhibit Erk2^{WT} (K_i >10,000 nM), the EC_{50} value shown is due to direct inhibition of MEK2. Because inhibitor **3** more potently inhibits the phosphorylation of Erk2^{WT}'s activation loop (EC_{50} = 390 nM) compared to Erk2^{DS2}'s activation loop (EC_{50} = 840 nM), the observed inhibitory effect is most likely due to direct inhibition of MEK2 rather than through this inhibitor's interaction with the drug-sensitized Erk2 mutant. N/D: not determined.

Data collection[a]	
Space group	P 1
Unit cell dimensions	a = 46.09 Å, b = 57.63 Å, c = 68.00 Å α = 86.57°, β = 88.98°, γ = 81.05°
Wavelength (Å)	0.97950
Resolution (Å)	67.88 – 2.20 (2.32 – 2.20)
Unique reflections	27949 (4179)
R_{pim}	0.099 (0.462)
Mean I/σ(I)	4.2 (1.5)
Completeness	79.8 (82.1)

Multiplicity	1.8 (1.8)
Wilson B-factor ($Å^2$)	35
Refinement	
Resolution (Å)	2.20
Reflections (working set)	26534
Reflections (test set)	1399
R_{work} / R_{free}	0.221 / 0.253
Protein atoms	5512
Inhibitor atoms	64
Water molecules	83
Other atoms	0
TLS groups	**A:** 8-13, 14-24, 25-34, 35-59, 60-74, 75-91, 92-97, 98-107, 108-158, 159-173, 174-187, 188-198, 199-205, 206-223, 224-274, 275-311, 312-328, 329-338, 339-346, 347-356 **B:** 8-34, 35-59, 60-75, 76-92, 93-97, 98-116, 117-122, 123-168, 169-174, 187-198, 199-204, 205-215, 216-248, 249-261, 262-272, 273-285, 286-310, 311-328, 329-339, 340-356
RMSD bond length (Å)	0.006
RMSD bond angles (°)	1.031
Ramachandran statistics	
In prefered regions	94.6%
In allowed regions	4.2%
Outliers	1.2%

[a]Values in parentheses are for highest resolution shell

Table S2, related to Figure 5. Data collection and structure refinement summary

	EC_{50} (nM)			
	1	**2**	**3**	**SB302580**
$Erk2^{WT}$	N/D	>10000	>10000	>10000
$Erk2^{DS2}$	N/D	< 20 (45%)	72 ± 6 (-41%)	< 20 (-21%)
p38α	25 ± 7 (76%)	N/D	N/D	190 ± 40 (-46%)

Table S3, related to Figure 6. Phosphatase inhibition of Erk2 and p38α using the ligands shown in Figure 2B. Values in parentheses indicate average plateau levels. N/D: not determined.

SUPPLEMENTAL METHODS

Small molecule synthesis

General procedures. Kinases for *in vitro* experiments were expressed and purified as described.[1] SB203580 was purchased from LC Laboratories. Ligands **1**[3] and **2**[1] were made as described. All other reagents were purchased from commercial suppliers and used without further purification.

Synthesis of ligand 3. Unless otherwise noted, all reagents were obtained from commercial suppliers and used without further purification. NMR spectra were obtained on a Bruker AV-300 or -301 instrument at room temperature. Chemical shifts are reported in ppm and coupling constants in Hz. Mass spectra were obtained on a Bruker Esquire Ion Trap instrument.

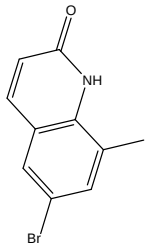

6-bromo-8-methylquinolin-2(1*H*)-one was made as described.[4]

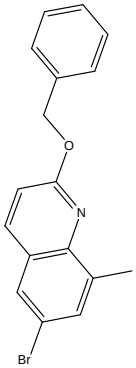

2-(benzyloxy)-6-bromo-8-methylquinoline: 6-bromo-8-methylquinolin-2(1*H*)-one (200 mg, 0.84 mmol), benzyl bromide (836 mg, 4.80 mmol), and Ag_2CO_3 (323 mg, 1.17 mmol) dissolved in dichloromethane (5 mL) were stirred at room temperature for 2 d. The reaction was then filtered through a bed of celite-545 powder that was washed with ethyl acetate (10 mL). The crude reaction mixture was subjected to flash chromatography using an EtOAc/hexanes solvent gradient. ^{1}H NMR (300 MHz, $CDCl_3$) δ 7.86 (d, J = 8.7 Hz, 1H), 7.70 (d, J = 2.1 Hz, 1H), 7.59 – 7.50 (m, 3H), 7.42 – 7.29 (m, 3H), 6.95 (d, J = 8.9 Hz, 1H), 5.55 (s, 2H), 2.68 (s, 3H); MS m/z ($C_{17}H_{14}BrNO$) calc'd = 327.0, observed: $[M+H]^+$ 328.4, 330.2 (Br doublet).

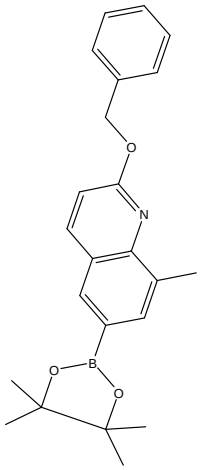

[A] 2-(benzyloxy)-8-methyl-6-(4,4,5,5-tetramethyl-1,3,2-dioxaborolan-2-yl)quinoline: This was made as described[5] (for the synthesis of "4c") using 2-(benzyloxy)-6-bromo-8-methyl-1,2-dihydroquinoline (23 mg, 0.07 mmol) as the halide starting material. The product was further purified by flash chromatography (0 – 90% EtOAc:Hex). ^{1}H NMR (300 MHz, $CDCl_3$) δ 8.09 (s, 1H), 7.98 (d, J = 8.9 Hz, 1H), 7.89 (s, 1H), 7.54 (d, J = 7.4 Hz, 2H), 7.46-7.24 (m, 3H), 6.92 (d, J = 8.7 Hz, 1H), 5.57 (s, 2H), 2.71 (s, 3H), 1.38 (s, 12H); MS m/z ($C_{23}H_{26}BNO_3$) calc'd = 375.2, observed: $[M+H]^+$ 376.6 and $[M+Na]^+$ 398.5.

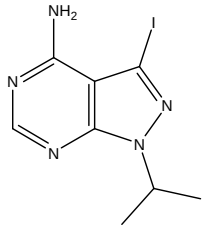

[B] 3-iodo-1-isopropyl-1*H*-pyrazolo[3,4-*d*]pyrimidin-4-amine was made as described.[6]

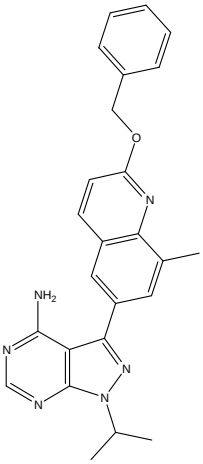

[3] 3-(2-(benzyloxy)-8-methylquinolin-6-yl)-1-isopropyl-1*H*-pyrazolo[3,4-*d*]pyrimidin-4-amine: This was made as described[6] ("General Suzuki coupling procedure" with RP-HPLC) using **A** (12 mg, 0.032 mmol) and **B** (9.7 mg, 0.032 mmol) as boronic ester and halide,

respectively, for a yield of 3.46 mg (25%). ^{1}H NMR (300 MHz, $CDCl_3$) δ 8.24 (s, 1H), 8.05 (d, *J* = 8.8 Hz, 1H), 7.83 (s, 1H), 7.75 (s, 1H), 7.56 (d, *J* = 7.2 Hz, 2H), 7.47 – 7.32 (m, 3H), 7.07 (d, *J* = 8.8 Hz, 1H), 6.31 (s, 1H), 5.61 (s, 2H), 5.29 – 5.12 (m, 1H), 2.80 (s, 3H), 1.66 (d, *J* = 6.8 Hz, 6H); MS m/z ($C_{25}H_{24}N_6O$) calc'd = 424.2, observed: $[M+H]^+$ 425.3.

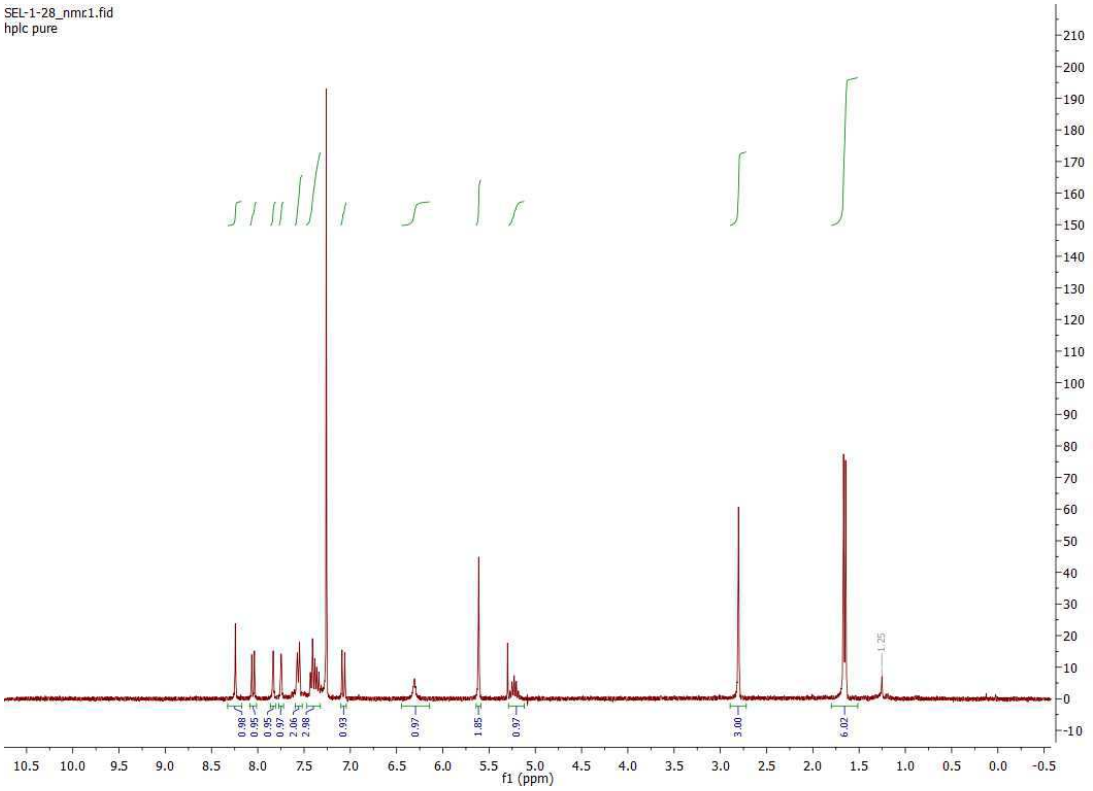

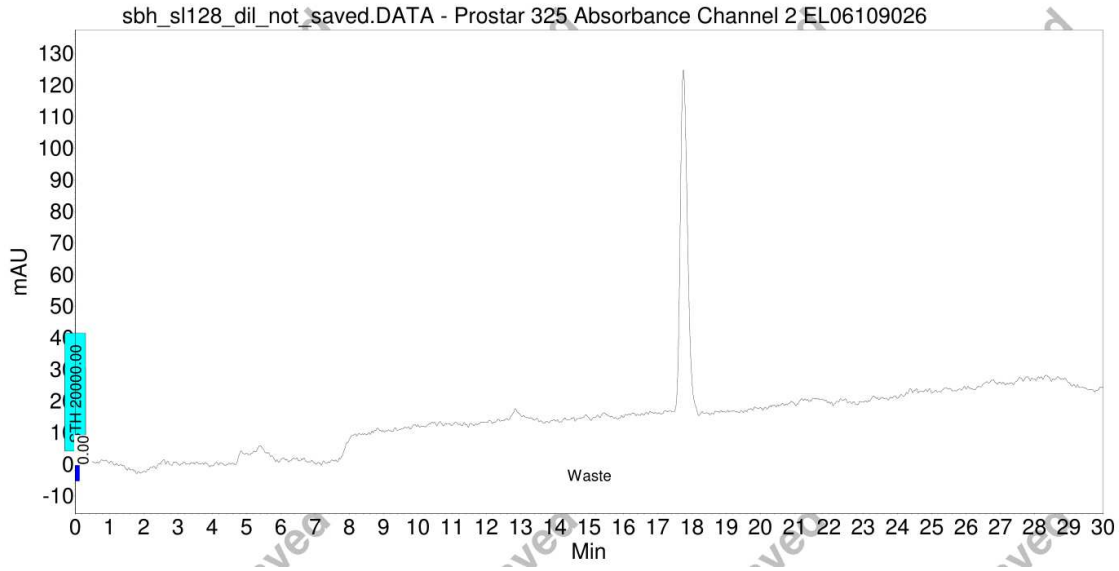

H_2O/Acetonitrile gradient

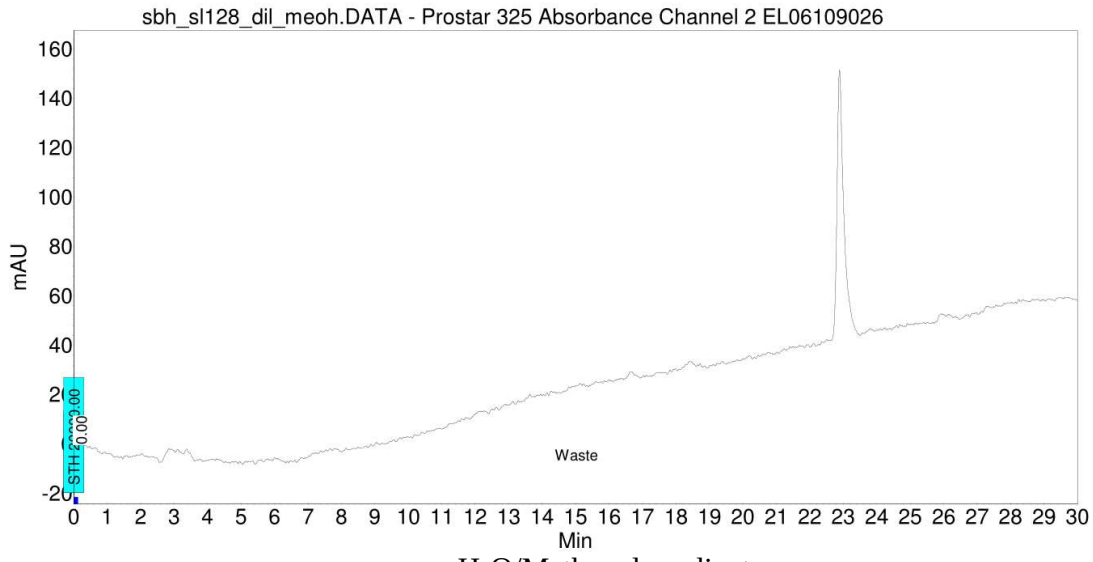

H_2O/Methanol gradient

Cloning and expression

MAPKs and MEKs. All MAPKs and MEKs used for *in vitro* assays were expressed and purified as described previously.[1]

eGFP-tagged kinases. The expression vector pcDNA-eGFP (#13031) was obtained through Addgene. A cassette containing an SspI site, linker, and ligation-independent cloning sites was inserted after the eGFP gene using site-directed mutagenesis.[7] An SspI site found elsewhere in the vector was removed by site-directed mutagenesis. The final vector was named pcEGFP-LIC. Genes coding $Erk2^{WT}$ and $Erk2^{DS1}$ were cloned into this vector using the ligation-independent cloning procedure described by Donnelly et al.[8]

DUSP6. Human DUSP6 (Addgene) was cloned into pMCSG7 (M. Donnelly) and expressed and purified with the same protocol used for kinases.[1]

DUSP10. Human DUSP10 (Open Biosystems) was cloned into pT7CFE1 and expressed using the 1-Step Human *In Vitro* Protein Expression Kit (Pierce) according to the manufacturer's instructions.

Crystallography

$Erk2^{DS2}$ was prepared as described previously.[1] Kinase was incubated with inhibitor **3** (final 1 mM in 5% DMSO) for 30 min at room temperature and centrifuged before setting up crystallization trials. Sparse-matrix screens Wizard I-IV (Emerald Biosciences) were used to find a condition that yielded plate crystals (0.1 M CHES pH 9.5, 30% PEG 3000) in five days, and crystals were harvested directly from the sparse-matrix plate. Diffraction images were collected at SSRL beamline 12-2 and processed using Mosflm[9] and the CCP4 program suite.[10] The initial structural model was found by molecular replacement[11] using PDB entry 3QYW and then subjected to alternating rounds of automated and manual refinement using REFMAC5[12] and Coot,[13] respectively. The final structure was deposited in the Protein Data Bank under accession code 4N4S.

SUPPLEMENTAL REFERENCES

1. Hari, S. B.; Merritt, E. A.; Maly, D. J., Sequence determinants of a specific inactive protein kinase conformation. *Chem. Biol.* **2013,** *20* (6), 806-15.
2. Sullivan, J. E.; Holdgate, G. A.; Campbell, D.; Timms, D.; Gerhardt, S.; Breed, J.; Breeze, A. L.; Bermingham, A.; Pauptit, R. A.; Norman, R. A.; Embrey, K. J.; Read, J.; VanScyoc, W. S.; Ward, W. H. J., Prevention of MKK6-Dependent Activation by Binding to p38α MAP Kinase. *Biochemistry* **2005,** *44* (50), 16475-16490.
3. Dumas, J.; Hatoum-Mokdad, H.; Sibley, R.; Riedl, B.; Scott, W. J.; Monahan, M. K.; Lowinger, T. B.; Brennan, C.; Natero, R.; Turner, T.; Johnson, J. S.; Schoenleber, R.; Bhargava, A.; Wilhelm, S. M.; Housley, T. J.; Ranges, G. E.; Shrikhande, A., 1-Phenyl-5-pyrazolyl ureas: potent and selective p38 kinase inhibitors. *Bioorg. Med. Chem. Lett.* **2000,** *10* (18), 2051-2054.
4. Alabaster, C. T.; Bell, A. S.; Campbell, S. F.; Ellis, P.; Henderson, C. G.; Roberts, D. A.; Ruddock, K. S.; Samuels, G. M.; Stefaniak, M. H., 2(1H)-quinolinones with cardiac stimulant activity. 1. Synthesis and biological activities of (six-membered heteroaryl)-substituted derivatives. *J. Med. Chem.* **1988,** *31* (10), 2048-56.
5. DiMauro, E. F.; Newcomb, J.; Nunes, J. J.; Bemis, J. E.; Boucher, C.; Buchanan, J. L.; Buckner, W. H.; Cee, V. J.; Chai, L.; Deak, H. L.; Epstein, L. F.; Faust, T.; Gallant, P.; Geuns-Meyer, S. D.; Gore, A.; Gu, Y.; Henkle, B.; Hodous, B. L.; Hsieh, F.; Huang, X.; Kim, J. L.; Lee, J. H.; Martin, M. W.; Masse, C. E.; McGowan, D. C.; Metz, D.; Mohn, D.; Morgenstern, K. A.; Oliveira-dos-Santos, A.; Patel, V. F.; Powers, D.; Rose, P. E.; Schneider, S.; Tomlinson, S. A.; Tudor, Y. Y.; Turci, S. M.; Welcher, A. A.; White, R. D.; Zhao, H.; Zhu, L.; Zhu, X., Discovery of aminoquinazolines as potent, orally bioavailable inhibitors of Lck: synthesis, SAR, and in vivo anti-inflammatory activity. *J. Med. Chem.* **2006,** *49* (19), 5671-86.
6. Johnson, S. M.; Murphy, R. C.; Geiger, J. A.; DeRocher, A. E.; Zhang, Z.; Ojo, K. K.; Larson, E. T.; Perera, B. G.; Dale, E. J.; He, P.; Reid, M. C.; Fox, A. M.; Mueller, N. R.; Merritt, E. A.; Fan, E.; Parsons, M.; Van Voorhis, W. C.; Maly, D. J., Development of Toxoplasma gondii calcium-dependent protein kinase 1 (TgCDPK1) inhibitors with potent anti-toxoplasma activity. *J. Med. Chem.* **2012,** *55* (5), 2416-26.
7. Bryksin, A. V.; Matsumura, I., Overlap extension PCR cloning: a simple and reliable way to create recombinant plasmids. *BioTechniques* **2010,** *48* (6), 463-5.
8. Stols, L.; Gu, M.; Dieckman, L.; Raffen, R.; Collart, F. R.; Donnelly, M. I., A New Vector for High-Throughput, Ligation-Independent Cloning Encoding a Tobacco Etch Virus Protease Cleavage Site. *Protein Expres. Purif.* **2002,** *25* (1), 8-15.
9. Leslie, A. G. W., Recent changes to the MOSFLM package for processing film and image plate data. *Joint CCP4 + ESF-EAMCB Newsletter on Protein Crystallography* **1992,** *26*.
10. Winn, M. D.; Ballard, C. C.; Cowtan, K. D.; Dodson, E. J.; Emsley, P.; Evans, P. R.; Keegan, R. M.; Krissinel, E. B.; Leslie, A. G.; McCoy, A.; McNicholas, S. J.; Murshudov, G. N.; Pannu, N. S.; Potterton, E. A.; Powell, H. R.; Read, R. J.; Vagin, A.; Wilson, K. S., Overview of the CCP4 suite and current developments. *Acta Crystallogr., Sect. D: Biol. Crystallogr.* **2011,** *67* (Pt 4), 235-42.
11. McCoy, A. J.; Grosse-Kunstleve, R. W.; Adams, P. D.; Winn, M. D.; Storoni, L. C.; Read, R. J., Phaser crystallographic software. *J. Appl. Crystallogr.* **2007,** *40* (Pt 4), 658-674.

12. (a) Murshudov, G. N.; Vagin, A. A.; Dodson, E. J., Refinement of macromolecular structures by the maximum-likelihood method. *Acta Crystallogr., Sect. D: Biol. Crystallogr.* **1997,** *53* (Pt 3), 240-55; (b) Murshudov, G. N.; Skubak, P.; Lebedev, A. A.; Pannu, N. S.; Steiner, R. A.; Nicholls, R. A.; Winn, M. D.; Long, F.; Vagin, A. A., REFMAC5 for the refinement of macromolecular crystal structures. *Acta Crystallogr., Sect. D: Biol. Crystallogr.* **2011,** *67* (Pt 4), 355-67; (c) Vagin, A. A.; Steiner, R. A.; Lebedev, A. A.; Potterton, L.; McNicholas, S.; Long, F.; Murshudov, G. N., REFMAC5 dictionary: organization of prior chemical knowledge and guidelines for its use. *Acta Crystallogr., Sect. D: Biol. Crystallogr.* **2004,** *60* (Pt 12 Pt 1), 2184-95.
13. Emsley, P.; Cowtan, K., Coot: model-building tools for molecular graphics. *Acta Crystallogr., Sect. D: Biol. Crystallogr.* **2004,** *60* (Pt 12 Pt 1), 2126-32.